SitR: Sitting Posture Recognition Using RF Signals

Lin Feng, Ziyi Li, Chen Liu, Xiaojiang Chen, *Member, IEEE*, Xiao Yin, and Dingyi Fang, *Member, IEEE*

***Abstract*—Sitting posture has a close relationship with our health, and keeping a healthy sitting posture is critical to each of us. Poor sitting postures often inevitably increase the risk of modern health musculoskeletal disorders. Previous works either used a camera to record the image or attached wearable sensors on the human body to recognize sitting postures. However, video-based approaches may face privacy issues while the wearable sensor-based approaches may cause uncomfortable to the user. In this work, we propose SitR, the first sitting posture recognition system using RF signals alone, which neither compromises the privacy nor requires wearing various sensors on the human body. We demonstrate that SitR can successfully recognize seven habitual sitting postures with just three lightweight and low-cost RFID tags pasted to the user's back. Our design exploits the correlation between the phase change of RFID tags and the sitting postures. By extracting effective features of the measured phase sequences and employing appropriate machine learning algorithm, SitR can achieve robust and high performance. We evaluate the performance of SitR with ten volunteers in two different scenarios. Extensive experiments show SitR can recognize seven sitting postures with a high accuracy across different scenarios and various conditions. SitR can further detect the abnormal respiration, stand up, and sit down and provide sitting posture history for sedentary people.**

***Index Terms*—RFID, sitting posture recognition.**

I. Introduction

TODAY, people of all ages have poor sitting postures for a long time due to their work or excessive dependence on electronic products. Poor sitting posture can negatively affect a human's mood and breath rhythm, making people fatigue [2]–[4]. It was reported that most sedentary people spent 54.9% of their working time in sedentary behaviors [5]. In fact, sedentary behaviors [6], [7] and poor sitting postures are closely related to modern health musculoskeletal disorders [8], [9], such as cervical spondylosis, chronic back pain, joint and muscle pain, improper spine alignment, and spine discs damage [10]–[14]. Diagnosing these diseases requires the long-term sitting posture monitoring, which can provide useful information for the doctor. The risk of these diseases would be less if people could properly control or reduce the time of nonvertical sitting posture. Therefore, reminding people to maintain a healthy sitting posture is significant.

Typically, sitting posture recognition approaches can be divided into two categories: 1) video-based approach and 2) wearable sensor-based approach. The video-based approaches require a camera to record the video streams and identify different sitting postures using the computer vision graphics processing [15]–[19]. Generally, these approaches mainly employ Kinect to extract features which can be further used as the input of the machine learning algorithm, whose recognition accuracy is high. However, video-based solutions may cause privacy concerns and require good lighting conditions. Although their accuracy is high, the privacy concern is a big issue, especially in a private environment. In contrast, the wearable sensor-based approaches [20]–[24] can recognize sitting postures without compromising the privacy. However, most of the approaches require the user to wear multisensors on his/her body, which is uncomfortable for long-term use. Also, some products for correcting the sitting postures, such as vibocare [25], are popular among young people. However, wearing this kind of product is uncomfortable and it cannot provide useful information (e.g., the sitting posture history in the long term) for diagnosing diseases. Here, we ask the following question: can we recognize sitting postures in a way that neither compromises the privacy nor requires wearing various sensors on the human body?

This article introduces SitR, the first sitting posture recognition system using only three lightweight and low-cost RFID tags pasted to the user's back (i.e., pasting to one's clothes). SitR can successfully recognize seven habitual sitting postures, including sitting straight (SS), lean forward (LF), lean backward (LB), left hand holding face (LHHF), right hand holding face (RHHF), fold right leg (FRL), and fold left leg (FLL) (see Fig. 1). Note that some recent works use WiFi signals to recognize human gestures or activities. SitR is different from these works in terms of the deployment strategy and the extracted features (parts of this work have been published in [1]; more details are discussed in Section II).

Manuscript received February 15, 2020; revised May 27, 2020 and July 10, 2020; accepted August 9, 2020. Date of publication August 25, 2020; date of current version December 11, 2020. This work was supported in part by the National Natural Science Foundation of China under Grant 61602382, Grant 61772422, Grant 61572402, Grant 61672428, and Grant 62061146001; in part by the Science and Technology Innovation Team Support Project of Shaanxi Province under Grant 2018TD-026; and in part by the International Science and Technology Cooperation Project under Grant 2019KWZ-05. This article was presented in part at the IEEE Pacific Rim Conference on Communications, Computers and Signal Processing, Canada, August 2019. *(Corresponding author: Ziyi Li.)*

Lin Feng and Xiao Yin are with the Shaanxi International Joint Research Centre for the Battery-Free IoT, Northwest University, Xi'an 710127, China (e-mail: lynnefeng@163.com; yinxiao@stumail.nwu.edu.cn).

Ziyi Li is with the Northwest University-Jingdong Wisdom Cloud Joint Research Center for AI & IoT, Northwest University, Xi'an 710127, China (e-mail: lzy_nwu@163.com).

Chen Liu is with the Northwest University Internet of Things Research Institute, Northwest University, Xi'an 710127, China, and also with the Department of Electrical and Computer Engineering, University of Victoria, Victoria, BC V8P 5C2, Canada (e-mail:liuchen@nwu.edu.cn).

Xiaojiang Chen is with the Shaanxi International Joint Research Centre for the Battery-Free IoT and the Northwest University-Jingdong Wisdom Cloud Joint Research Center for AI & IoT, Northwest University, Xi'an 710127, China (e-mail: xjchen@nwu.edu.cn).

Dingyi Fang is with the Shaanxi International Joint Research Centre for the Battery-Free IoT and the Internet of Things Research Institute, Northwest University, Xi'an 710127, China (e-mail: dyf@nwu.edu.cn).

Digital Object Identifier 10.1109/JIOT.2020.3019280

Fig. 1. Seven habitual sitting postures. (a) SS. (b) LF. (c) LB. (d) LHHF. (e) RHHF. (f) FRL. (g) FLL.

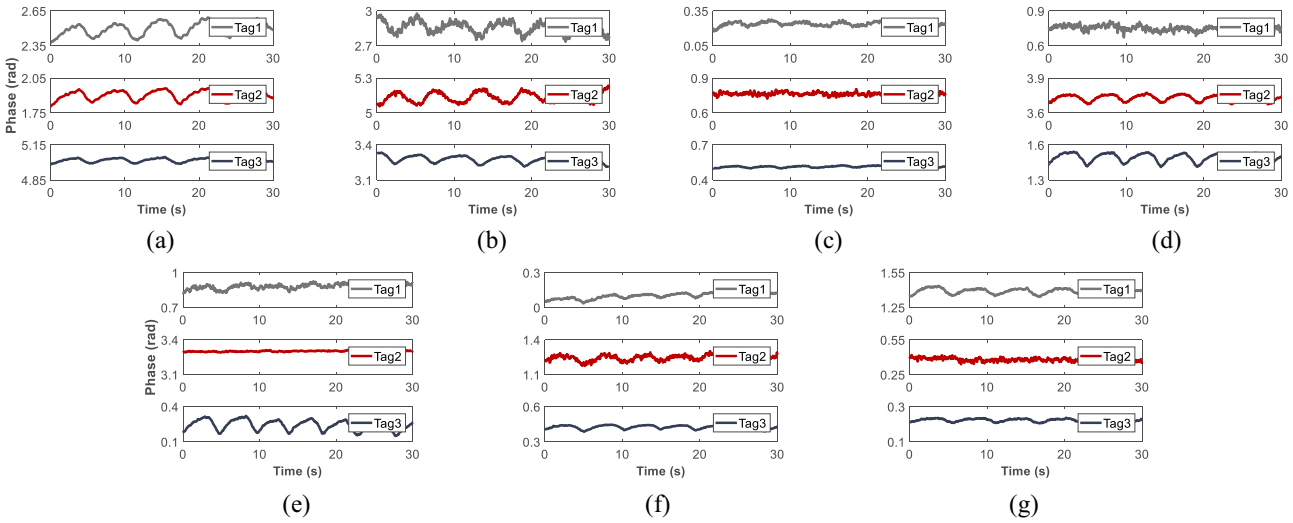

Fig. 2. Phase of seven habitual sitting postures. (a) SS. (b) LF. (c) LB. (d) LHHF. (e) RHHF. (f) FRL. (g) FLL.

The basic idea of SitR is as follows: 1) with three tags pasted to the user's back and the antenna placed on the back of the chair. The distance between each tag and the antenna varies under different sitting postures; 2) when the distance and angle of the tag to antenna changes, the received signal phase at the reader changes accordingly. Note that the phase variation for different sitting posture is unique, which can be used as a reliable primitive for sitting posture recognition (see Fig. 2); and 3) besides, these three tags can sense the user's respiration and we find that the observed respiration patterns from the measured phase sequences are distinct under different sitting postures. Therefore, SitR can recognize sitting postures by carefully processing the measured phase sequences without compromising the privacy nor wearing various sensors. Although the basic idea of SitR sounds straightforward, there are three challenges to realize the system.

1) The first challenge is how to deploy the tags to effectively recognize the sitting postures without bringing uncomfortable experience to the user. To deal with this challenge, we find that pasting tags on one's back is sufficient to capture effective information for distinguishing sitting postures, while keeping unaware to the user. At the same time, we also verified the influence of the number of tags on the recognition accuracy. We use only three tags to capture the phase information in three key regions of the spine, which achieves a high recognition accuracy.
2) The second challenge is how to obtain an obvious phase changing pattern in the presence of hardware noise and multipath effect. To solve this problem, we propose a data preprocessing method to remove the outliers and eliminate the multipath effect.
3) The last challenge is how to extract effective features from the phase measurements to represent sitting postures to achieve high accuracy. By jointly considering the features from the time domain and frequency domain, SitR can successfully recognize sitting postures in both person-dependent and person-independent scenarios.

We implement and evaluate SitR through extensive experiments, including ten volunteers in the classroom and office scenarios. The result shows that SitR can recognize sitting postures with an average accuracy of 98.83%. Our system can further detect the abnormal respiration, stand up, and sit down and provide sitting posture history for sedentary people. This article makes the following main contributions.

1) We introduce the first sitting posture recognition system using only three lightweight and low-cost RFID tags pasted to the user's back. SitR has a higher recognition accuracy without compromising the privacy nor wearing various sensors.
2) We propose a phase-shift calibration algorithm to remove the hardware noise, and the activity detection algorithm to detect "stand up" and "sit down" activities. The method of sitting posture recognition in SitR can be applied in many RFID sensing applications (i.e., respiration monitoring).
3) We evaluate the performance of real-world environment and through extensive experiments with ten volunteers

in two scenarios. The results show that SitR can recognize human's sitting posture at an average accuracy of 98.83%. Besides, we evaluate the performance on different antenna gains, the material of the chair, the thickness of clothes, and the number of tags to validate the system robustness.

II. Related Work

SitR is related to the following existing works.

Video-Based Approach: The video-based approaches require a camera to record the video streams and identify different sitting postures using computer vision graphics processing. However, the privacy concern is a big issue, especially in a private environment.

Edmond *et al.* [15] used the camera to capture 3-D postures and classified the postures with a max-margin classifier. The system only recognizes three sitting postures with an accuracy of 79.45%. Poor sitting posture was recognized in [16] mainly by the measurement of the neck and the torso angle, which were extracted based on the depth image using the Kinect sensor. The average accuracy of sitting posture recognition is about 93.3% under different conditions. However, the accuracy of "sitting with body moving" is only 73.3%, and the posture cannot be recognized if the user moves frequently. Weidong *et al.* [17] fused the relevant features in the scene and the bone features extracted from the human body into the semantic features to distinguish various sitting postures. However, the method depends on the objects in the environment and good lighting conditions.

Pujana *et al.* [18] used a single Kinect camera to capture the skeleton data and several classification methods to recognize sitting postures for office workers. This system used two devices, Kinect and alarm device, were separately used to recognize the sitting posture and monitor the sitting time. But it is inconvenient to use two devices in real sitting posture recognition applications. Lan *et al.* [19] extracted profile features through pattern matching based on the Hausdorff distance and designed a surveillance system for human sitting postures. However, the method would fail with bad light intensity.

Wearable Sensor-Based Approach: The wearable sensor-based approaches can recognize sitting postures without compromising the privacy. They mainly used sensors to extract the feature of different sitting postures.

Sangyong *et al.* [20] used a three-axis accelerometer which was connected to the back of the user to retrieve the acceleration data. Acceleration data were transformed to the feature vectors of principal component analysis. Support vector machine (SVM) and *K*-means clustering were used to classify sitting posture with the transformed feature vectors. Jheanel and Larry [21] used three gyroscopes worn on the user's back to recognize the sitting postures. The data from gyroscopes were being collected by the mobile devices connected to the gyroscopes. Corinne *et al.* [22] used a thermoplastic elastomer strain sensor to measure strain in clothes, and then recognized different postures by the naive Bayes classifier.

Yong-Ren and Xu-Feng [23] fixed positions of force sensors on the seat cushions and obtain the information of the sitting postures from the circuits on the microcontroller. The method recognized the sitting posture by categorizing the information. Congcong *et al.* [24] proposed a cushion-based posture recognition system that was used to process pressure sensor signals for the detection of the user's posture in the wheelchair. Compared with the wearable sensors, an RFID tag used in SitR is lightweight (i.e., like a piece of paper) and does not need any battery, which is proper for long-term use.

TABLE I
Summarization of the Existing Sitting Posture Recognition Methods

System	Technique	Method	Accuracy
[15]	Kinect	maxmargin classifier	79.45%
[16]	Kinect2.0	Neck/Torso angle	93.3%
[17]	Kinect	Faster RCNN	95.6%
[18]	Kinect	Decision Tree	98.04%
[20]	Axis accelerometer	SVM	95.33%
[21]	Mobile devices	Decision Tree	96.13%
[22]	Strain sensors	Bayes	97%
[24]	Smart cushion	Decision Tree	99.47%

To show a clear comparison, we summarize the above sitting posture recognition methods in terms of the technique and accuracy in Table I.

WiFi-Based Gesture Recognition: Many recent works use WiFi signals to recognize human gestures, including arm motions (e.g., push, pull, flick, circle, down-up, and up-down [26]–[29], hand gestures (e.g., keystroke and finger-grained gestures [30], [31]), and daily activities (e.g., running, walking, falling, and brushing [32], [33]). Both our solution and WiFi-based solutions employ the change of the wireless signals caused by the human body/arm/hand to recognize gestures or activities. However, there are two main differences between our solution and WiFi-based solutions. First, the deployment strategy is different. Most WiFi-based gesture recognition solutions deployed a pair of Tx and Rx in a room. While this deployment strategy works well for arm/hand gesture or activity recognition, it is challenging to capture the useful information from a person's back/spine. Second, the extracted features are different. The existing WiFi-based gesture recognition systems focused on detecting the dynamic motions, such as the hand/arm/body movements. Thus, features, such as the speed, the start/end point, and the motion duration, are widely used. However, these dynamic features cannot be directly applied for sitting posture recognition since the sitting posture is almost static. Different from the existing WiFi-based gesture recognition, SitR employs only three lightweight and low-cost RFID tags pasted to the user's back and extracts effective features from both the time domain and frequency domain to recognize the sitting postures.

III. Preliminary

The commodity passive RFID system, including RFID reader, RFID antenna, and RFID tag. As shown in Fig. 3, the reader sends an RF signal to the space through the antenna. The tag in the electromagnetic field receives the RF signal to generate an induced current, which activates the tag. The tag then feeds back its ID information to the antenna through the backscattered signal. Besides the ID, the reader also measures

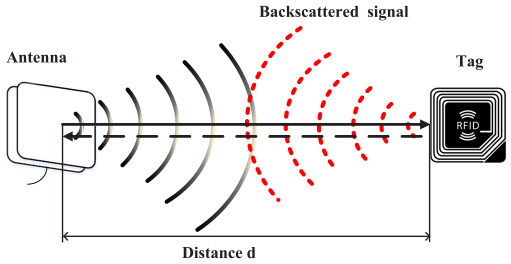

Fig. 3. Passive RFID system.

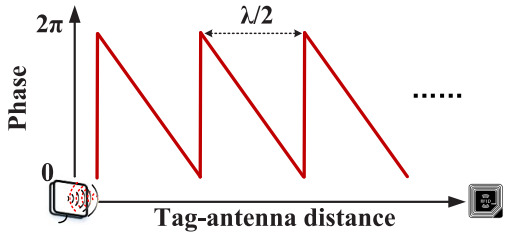

Fig. 4. Relationship between distance and phase value.

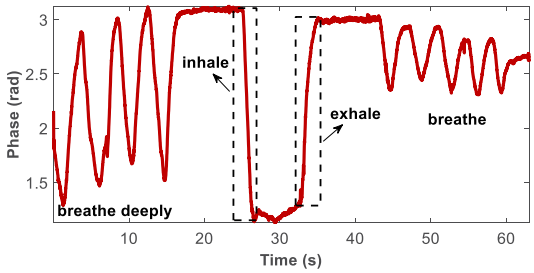

Fig. 5. Phase change of breath.

the strength and phase of the received signal after demodulation and decoding. In SitR, we mainly use phase information to recognize the sitting postures since the commodity RFID reader needs to be able to output very fine-grained phase information.

A. Relationship Between Phase and Distance

Suppose the distance between the antenna and tag is d (see Fig. 3) and the RF signal propagates along the direct path. The received phase sequence at the reader can be written as follows:

$$\phi = \left(\frac{2\pi}{\lambda} \times 2d + \Omega\right) \bmod 2\pi \tag{1}$$

$$\Omega = \Omega_s + \Omega_n \tag{2}$$

where λ is the wavelength of the signal, and Ω is the phase offset caused by the hardware circuits which is a constant phase shift Ω_s and the random hardware phase noise Ω_n. Thus, we can know that the received phase sequence ϕ is a function of d and disturbed by Ω.

We then conduct an experiment for verifying the relationship between phase and distance. Fig. 4 shows that the phase values gradually decrease from 2π to 0 and periodically repeat when the tag moved far from the antenna. The value of the phase depends on the distance between the tag and antenna. We define the distance between three tags and antenna as $d1$, $d2$, and $d3$ (in the order of one's back from top to bottom), respectively. The three distances are different from different sitting postures. For example, the relationship of the three distances in leaning forward is $d1 > d2 > d3$, while it is usually just the opposite in leaning backward. When the tag rotates at different angles with the user's back, the tag-to-antenna distance of seven sitting postures is different, which in turn changes the phase change of tags [34]. We can measure the phase readings of tags from different sitting postures. As shown in Fig. 2, we can see that the phase sequence of seven different sitting postures is totally different.

B. Breath Detection Under Different Sitting Postures

We paste three tags on one's back to recognize the seven different sitting postures and find that the tags can sense the breath of the user. The phase sequence changes according to the undulations of the chest. As shown in Fig. 5, the volunteer has a deep breath first → hold her breath → inhale → hold her breath → exhale → hold her breath → breath. We define the distance difference between the chest and the antenna as Δd when the volunteer exhale/inhale. The phase change $\Delta\phi$ can be written as

$$\Delta\phi = \left(\frac{2\pi}{\lambda} \times 2\Delta d + \Delta\Omega\right) \bmod 2\pi \tag{3}$$

according to (1), and we can get the following equation if ignoring $\Delta\Omega$:

$$\frac{\Delta\phi}{\Delta d} = \frac{4\pi}{\lambda}. \tag{4}$$

We can see that the measured phase sequence is almost unchanged when she holds her breath ($\Delta d \approx 0$ and $\Delta\phi \approx \Delta\Omega$). The phase change of the deep breath is more than normal breath. Because deep breath causes greater undulations in the chest [35], Δd is larger, and $\Delta\phi$ is proportional to Δd according to (4).

Only SS is diaphragmatic breathing (or deep breathing, which is achieved by contracting the diaphragm), which is the healthiest breathing [36]. Poor sitting postures (bending forward, backward, or sideways) invite distorted/restricted/shallow breathing, and long-term poor sitting postures invite suppressed breathing [37]. For example, the phase change of Tag1 in LF posture [see Fig. 2(b)] is not as clear as that in the SS posture. Fig. 2(a) shows that the SS posture obtains the "clearer" phase change from the three tags. We suppose that the user remains one sitting posture for a while, and the phase changes of the three tags are constant according to (3). However, the phase changes of three tags are different in the different sitting postures. Fig. 2 shows that the phase changes of seven separate sitting posture are distinguishable.

IV. SitR Design

SitR employs just three low-cost and lightweight RFID tags pasted to a user's back and a reader antenna placed on the back of a chair to recognize seven habitual sitting postures, and we achieve high performance for sitting posture recognition through detailed system design. As shown in Fig. 6,

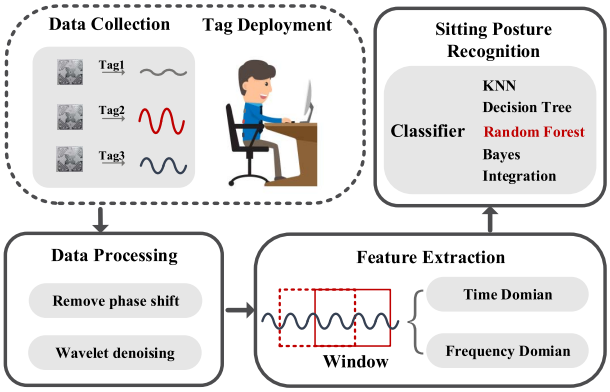

Fig. 6. System flow of SitR.

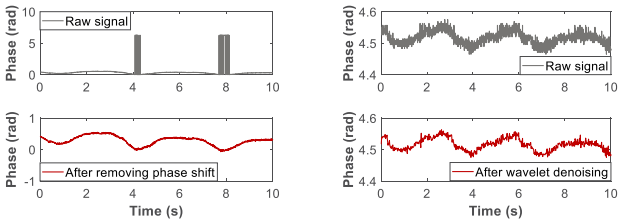

Fig. 7. Data preprocessing. (a) Phase shift calibration. (b) Wavelet denoising.

there are four steps in SitR: 1) tag deployment and data collection; 2) data preprocessing; 3) feature extraction; and 4) sitting posture recognition.

A. Tag Deployment and Data Collection

The lightweight and low-cost RFID tags are widely used in many applications [38]–[41], and one of the important reasons is the convenient deployment of the tag. We find that pasting tags on one's back is sufficient to capture effective information for distinguishing sitting postures, while keeping unaware to the user. The position and shape of the spine will change according to the change of the sitting postures [42]. Especially, the common asymmetric sitting postures on spinal balance will cause spinal imbalances and injuries [43]. So we paste tags on the three key regions of the spine, including the thoracic, thoracolumbar, and lumbar, which are also the key positions of human's back in sitting posture recognition [21].

However, how many tags should we use in SitR to capture the information of the sitting posture? When two RFID tags are placed close to each other, mutual coupling will change the radiation pattern of the tag antenna, affecting the received phase sequence [34], [39], [41]. The distance between adjacent tags should be set more than 5 cm to avoid the coupling interference. We set the distance between two neighbor tags is around 10 cm in our experiments. Note that this distance may vary slightly for different users due to their heights and the positions of the three key regions. In order to avoid the interference, the number of tags is minimized as much as possible while ensuring high performance. We evaluate the performance with different number of tags in Section V. We finally use three tags that can capture enough effective information of the spine, and achieve a high performance. We then extract the phase information from the signals of the three tags received by the reader.

Algorithm 1 Phase Shift Calibration

Input: Raw phase sequence X and a set of template sequences X_0, X_1, ..., X_i, ..., X_N.
Output: Phase sequence after removing phase shifts

Calculate the average (μ) and length (N) of X
for i=2:N **do**
  dif1 $= abs(\mu - X(i-1))$;
  dif1 $= abs(\mu - X(i))$;
  if $abs(X(i) - X(i-1)) > 2 * \pi$ **then**
    if dif1 <= dif2 **then**
      if $X(i-1) <= X(i)$ **then**
        $X(i) = X(i) - 2 * \pi$
      else
        $X(i) = X(i) + 2 * \pi$
    if dif1 > dif2 **then**
      if $X(i-1) <= X(i)$ **then**
        $X(i-1) = X(i-1) + 2 * \pi$;
      else
        $X(i-1) = X(i-1) - 2 * \pi$;
  else if $abs(X(i) - X(i-1)) > \pi$ **then**
    if dif1 <= dif2 **then**
      if $X(i-1) <= X(i)$ **then**
        $X(i) = X(i) - \pi$
      else
        $X(i) = X(i) + \pi$
    if dif1 > dif2 **then**
      if $X(i-1) <= X(i)$ **then**
        $X(i-1) = X(i-1) + \pi$;
      else
        $X(i-1) = X(i-1) - \pi$;
return X

B. Data Preprocessing

The in-air raw signals from RFID devices are noisy due to the hardware imperfection and multipath effect, which may cause false edges and affect the recognition accuracy. We therefore propose a two-step data preprocessing method to filter out the noise.

The first step is to remove the phase shift Ω caused by the hardware. For an RFID system, the reader emits the RF signals through the antenna, and then the tag receives the signals and feeds them back to the reader. There exists a constant phase shift of π or 2π caused by hardware circuits [40]. For example, the top figure in Fig. 7(a) shows an arbitrary sequence of the phase measurements from the RFID system. As we can see, there are phase shifts of 2π around 4th and 8th seconds, respectively. We can also observe the phase shifts of π in other arbitrary measurements. To remove the phase shift caused by hardware circuits, we compare the two adjacent phase measurements and apply a threshold to detect and then calibrate the phase shift. Note that this threshold should be consistent with the constant phase shift value (i.e., π or 2π)

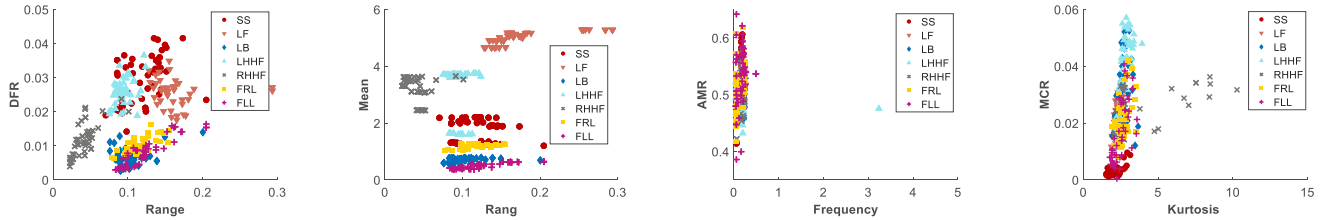

Fig. 8. Feature distribution. (a) DFR and range. (b) Mean and range. (c) AMR and frequency. (d) MCR and kurtosis.

caused by hardware circuits. Accordingly, we set the threshold as π or 2π. The detection and calibration procedure can be described as follows. If the phase difference between the two adjacent measurements exceeds a threshold of π or 2π, we calibrate the phase shift by subtracting/adding π or 2π to the outlier. The bottom figure in Fig. 7(b) shows the calibrated phase measurements. The details of the phase-shift calibration algorithm is shown in Algorithm 1.

In a real indoor environment, the received signal is a combination of the line-of-sight (LOS) signal and multipath signals reflected from objects in the environment. So the second step is to eliminate the multipath effect from the indoor environment. We employ the wavelet denoising filter (i.e., Daubechies 2 wavelet) to remove the high-frequency noise in the measured phase sequence. Fig. 7(b) shows the measured phase values before and after wavelet denoising.

C. Feature Extraction

The key part of SitR is to extract rich features of the phase sequences to represent different sitting postures. Intuitively, we can use the features that are widely used in RF-based activity recognition systems [18], [38], [44]. However, how to choose the representative features to recognize sitting postures with a high accuracy?

To do so, we analyze the distribution of each feature both within the same sitting posture and across different postures. We select the features that have large variations on different sitting postures while keep stable within the same posture. Conversely, features that do not have the above characteristic are likely to cause interference in sitting posture recognition, and we avoid selecting such features. For example, Fig. 8 shows the feature distribution of the seven sitting postures.[1] Fig. 8(a) shows that the feature distribution of the same sitting posture is gathering, and the feature distribution of dominant frequency ratio (DFR) and range can separate seven sitting postures into three clusters.[2] Fig. 8(b) shows that feature mean can well separate SS and LF postures of the first cluster and distinguish "FRL" and FLL postures of the second cluster. However, Fig. 8(c) and (d) shows that the feature distribution of AMR, frequency, MCR, and kurtosis are overlapping, which cannot well distinguish the seven sitting postures. We find that features like these four features are confusing rather than help with each other. Thus, we need to exclude the features that do not contribute to the accuracy.

[1]The abbreviations of seven sitting postures are as follows: "sitting straight (SS)," "lean forward (LF)," "lean backward (LB)," "left hand holding face (LHHF)," "right hand holding face (RHHF)," "fold right leg (FRL)," and "fold left leg (FLL)."

[2]The first cluster includes SS, LHHF, and LF postures, the second cluster includes FRL, FLL, and LB postures, and RHHF is the sole posture in the third cluster.

TABLE II
EFFECTIVE FEATURES IN SITR

Basic properties of signals	Feature
Time Domain	Variance (σ)
	Periodic Reversal (Pr)
	Mean (μ)
	Range (Δ)
Frequency Domain	Dominant Frequency Ratio (DFR)
	Energy (E)
	Entropy (H)

Eventually, SitR selects seven effective features shown in Table II as the input of the sitting posture recognition model. Note that the users have different frequencies and speeds when switching between the different sitting postures. In order to obtain the sitting posture information more accurately, we use a sliding window to divide the phase sequence into several segments, and the overlapping rate as 50%. We then extract the features for each segment.

The seven effective features describe the characteristics of the phase sequences in the time domain and frequency domain, and they obtain enough information about the seven sitting postures to distinguish each other. In detail, the mean (μ) is defined as the average of the phase sequence, while variance (σ) and range (Δ) are used to quantify the magnitude of the phase change caused by breath. The energy (E) represents the signal strength and is defined as

$$E = \sum_{i=1}^{N} m^2 \tag{5}$$

where m is the magnitude of FFT coefficients, and N is the size of a sliding window. We define the amount of information in the signal, denoted as entropy (H)

$$H = -\sum_{i=1}^{N} n_i \log_2(n_i) \tag{6}$$

where n_i is the normalized value of FFT coefficients.

There are differences in the periodicity of the measured phase sequence in seven sitting postures. Periodic reversal (Pr) and DFR can well describe the periodicity of phase sequence. We can model the measured phase sequence as a sinusoidal wave when detect the user's breath. We argue that the larger

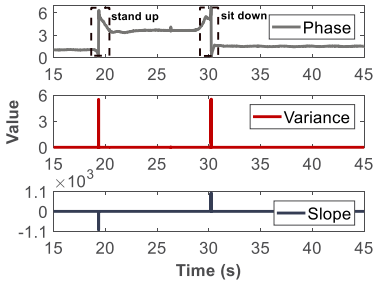

Fig. 9. Detection of stand up and sit down.

the amplitude of the identified sinusoidal wave, the higher the periodicity level [45]. The measured phase sequence $x(t)$ can be modeled as a sinusoidal wave

$$x(t) = A\sin(2\pi ft + \Omega_0) + D + n_0(t) \tag{7}$$

where the constants A, f, and Ω_0 are the amplitude, frequency, phase, and shift of the identified sinusoidal wave, and n_0 is an additive noise. The goodness of fit can be calculated by the root-mean-square error (RMSE) defined as

$$\text{RMSE} = \sqrt{\frac{1}{N}\sum_{i=1}^{N}\big(\hat{x}(t) - x(t)\big)^2} \tag{8}$$

where $\hat{x}(t)$ is predicted values at time t using the sinusoidal model and $x(t)$ is a measured phase sequence. N is the length of the $x(t)$. We define the periodicity level of an $x(t)$, denoted as Pr, as the ratio of the two parameters

$$\text{Pr} = A/\text{RMSE}. \tag{9}$$

DFR is also a vital feature, in frequency domain, to measure the periodicity. It is calculated as

$$\text{DFR} = \frac{m_{f_r}}{E} \tag{10}$$

where f_r is the dominant frequency and m_{f_r} is the amplitude of f_r.

D. Sitting Posture Recognition

The machine learning method is widely used in wireless sensing applications [46]–[48]. After extracting the effective features from the measured phase sequences of the three tags for seven sitting postures, SitR employs the random forest classifier to recognize sitting postures. In fact, other widely used classifiers, such as decision tree (D-Tree), Bayes, K-nearest neighbor (KNN), and integration learning are used as well. Here, we choose the random forest classifier just because it can achieve high performance without complicated parameter adjusting.

There are some activities that are inseparable from the sitting posture, such as standing up and sitting down. We also detect activities stand up and sit down in SitR. As shown in Fig. 9, we can observe an abrupt change in the phase sequence when the user stands up and sits down. Besides the abrupt change, it is easy to find that the slope of the phase sequence in stand up activity is negative, while the slope of the phase sequence in sit down activity is positive. However, the slope of the abrupt change in the phase sequences is contrary to the remaining phase sequences during the activities. In order to improve the accuracy of detection, we perform two steps.

1) We detect the two activities with the "variance," which is the sum of variances between the adjacent phase sequence during the activities. To prevent errors caused

Algorithm 2 Activity Detection Algorithm

Input: Labeled and preprocessed phase sequence X: X_0, X_1, ..., X_i, ...X_N. The time sequence T: T_0, T_1, ..., T_i, ...T_N. N is the length of X. **Output:** S: the sum of all slopes during the activities.

Define the temporary variable index1, index2, index3, and index4.
Calculate the variance(v) and slope(s) of adjacent phase sequence (i.e., X_1 and X_2).
for $i = 1 : N$ **do**
  if $i < N$ **then**
    index1 $= var([X(i)X(i+1)])$
    index2 $= (X(i+1) - X(i))/(T(i+1) - T(i))$
  else
    index1 $= var([X(i)X(i-1)])$
    index2 $= (X(i) - X(i-1))/(T(i) - T(i-1))$
  $v = [v : \text{index1}]$
  $s = [s : \text{index2}]$
Negate s when the v is more than 1.
for $i = 1 : N$ **do**
  if $v(i) > 1$ **then**
    $s(i) = -s(i)$
  else
    $s(i) = s(i)$
Define V to be the sum of all v during the activities.
Note that the length of the activities is about 400.
for $i = 1 : N$ **do**
  if $i < 200$ and $v(i) > 0.5$ **then**
    index3 $= v(i)$
  else if then$200 < i < N - 200$ and $v(i) > 0.5$
    index3 $= sum(v(i - 200 : i + 200))$
  else if then$N - 200 < i < N$ and $v(i) > 0.5$
    index3 $= v(i)$
  else
    index3 $= v(i)$
  $V = [V : \text{index3}]$
Define S to be the sum of all s during the activities.
for $i = 1 : N$ **do**
  if $i <= 200$ and $V(i) > 1$ **then**
    index4 $= sum(s(i : i + 400))$
  else if then$200 < i < N - 200$ and $V(i) > 1$
    index4 $= sum(v(i - 200 : i + 200))$
  else if then$N - 200 < i < N$ and $V(i) > 1$
    index4 $= sum(s(i - 400 : i))$
  else
    index4 $= 0$
  $S = [S : \text{index4}]$
return S

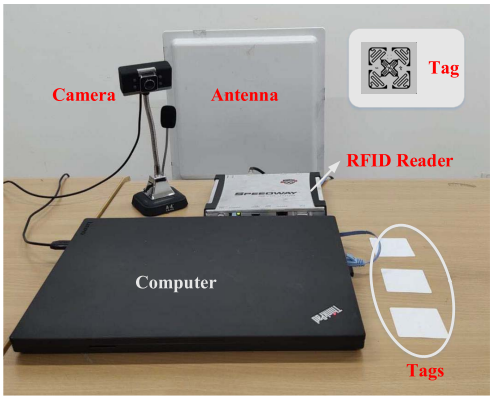

Fig. 10. Experimental equipment.

by other unknown body movement of the body, we sum variances that greater than an empirical threshold during the activity. Specifically, if the sum variance exceeds an empirical threshold, we can detect the activity of stand up or sit down. To set this empirical threshold properly, we analyzed all the collected samples of stand up or sit down from three volunteers in the same environment. To see it clearly, instead of analyzing the sum variance directly, we zoom in to the variance distribution for a given activity. We observed that during the time period of the given activity (either stand up or sit down), the maximum variance is larger than 1, while only several variances are less than 1 but larger than 0.5. In this case, we set the threshold of the sum variance as 1 to achieve high accuracy. Note that this threshold is from our empirical study with three volunteers in the same environment, and it worked well in our experiment. It may be slightly different for other experimental settings.

2) We then distinguish the activities with the "slope," which is the sum of slopes between the adjacent phase sequence during the activities. Especially, we reverse the slope of the abrupt phase. We can detect sit down when the value of the slope is more than zero and detect as stand up when the value of the slope is less than zero. The details of the activity detection algorithm are shown in Algorithm 2.

V. Evaluation

In this section, we first introduce the implementation of SitR, and then evaluate the system performance under various conditions, including different classifiers, scenarios, users, the number of tags, etc. Finally, we compare our system with the state-of-the-art work.

A. Implementation

1) Experimental Settings: As shown in Fig. 10, we implement SitR with three UHF passive Alien tags H47, an Impinj R420 RFID reader with a fixed frequency of 924.375 MHz, and an RFID directional antenna. The maximum transmission power of the RFID antenna used in this article is 30 dBm, and the maximum gain is 12 dBi. In this article, we set the transmission power of the RFID reader to 24 dBm. The reader is connected to a laptop through an Ethernet cable, and the laptop is used for data collection. The antenna is connected to the reader with UHF coaxial feeder and radiates outward the electromagnetic wave signal emitted by the reader. The tag receives and feeds back the signal to the reader. We also used a camera to record the ground truth and we labeled the sitting postures manually.

2) Data Collection: To evaluate SitR, we recruited ten volunteers, including four females and six males. Their ages are from 19 to 28 years old, with the height varying from 155 to 187 cm and weight from 46 to 70 kg. The volunteers sat naturally on the chair while studying/working/playing games. We pasted three tags on his/her back within three key regions of the spine, including the thoracic, thoracolumbar, and lumbar. Note that the three tags are not required to be precisely pasted to the same locations for different people. Roughly pasting them within the three key regions is enough to achieve high accuracy. The antenna is placed on the back of the chair at an angle of 90° to the ground.

To demonstrate the robustness of SitR in different environments, we evaluated the performance in two different scenarios, including an office and a classroom (see Fig. 11). We performed 2-h sitting posture monitoring for ten volunteers in the two scenarios, respectively. During the monitoring period, the volunteers performed the seven habitual sitting postures. In order to obtain long-term monitoring of performance and sitting habits, we let two of them monitor for 3 h. We have totally collected 20 949 samples from ten volunteers for sitting posture monitoring.

3) Parameters Configuration: The proposed sitting posture recognition method is programmed in MATLAB R2018b. Specifically, we set $K = 3$ for KNN classifier, standardize the input data, and use cityblock to be the distance metric. The number of decision trees is set as 50 for random forest classifier. For integration learning, we applied the widely used AdaBoostM2 algorithm. Meanwhile, we make the features obey the normal distribution (Gaussian) when training the multiclass naive Bayes classifier. For each volunteer, we divided his/her data into training set (4/5) and testing set (1/5), respectively. We trained/tested our model until all the samples are trained/tested at least once.

4) Evaluation Metrics: We use the cross-validation and employ four metrics, including the accuracy, F1 score, precision, and recall, which are widely used in machine learning field to evaluate the system performance [49]. The accuracy is the proximity of measurement results to the true value. The precision is the number of correct positive results divided by the number of all positive results returned by the classifier. The recall is the number of correct positive results divided by the number of all relevant samples (all samples that should have been identified as positive). The F1 score is a measure of a test's accuracy, which considers both the precision and the recall

$$\text{precision} = \frac{\text{TP}}{\text{TP} + \text{FP}} \tag{11}$$

$$\text{recall} = \frac{\text{TP}}{\text{TP} + \text{FN}} \tag{12}$$

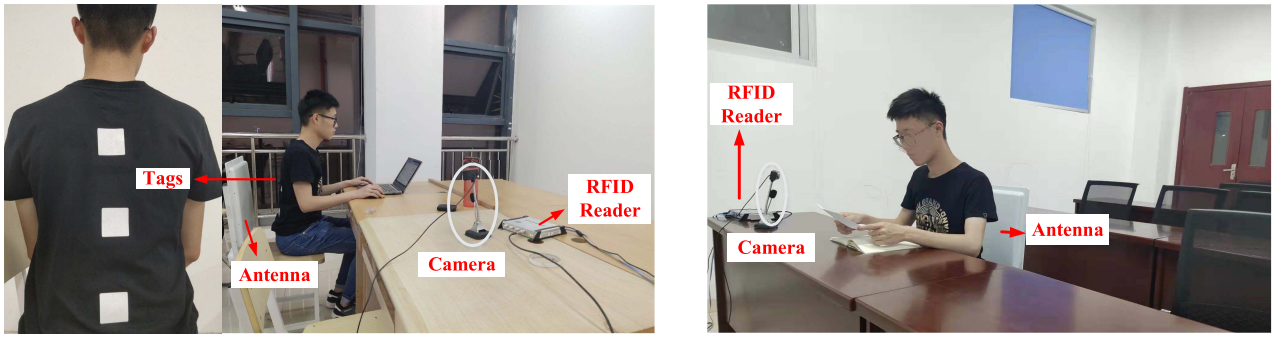

Fig. 11. Different scenarios. (a) Office scenario. (b) Classroom scenario.

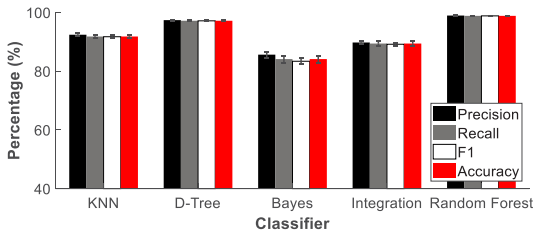

Fig. 12. Classifier comparison.

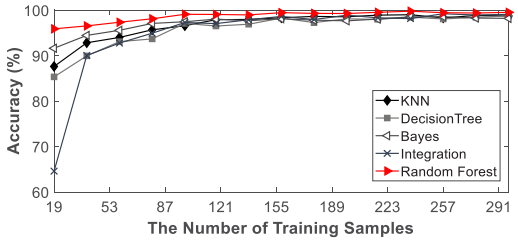

Fig. 13. Accuracy of different training samples.

$$\text{F1 score} = \frac{2 \times \text{precision} \times \text{recall}}{\text{precision} + \text{recall}} \tag{13}$$

where TP, FP, TN, and FN mean true positive, false positive, true negative, and false negative, respectively.

B. Evaluation Results

1) Performance of Classifiers: Fig. 12 shows the average precision, recall, F1 score, and accuracy of all volunteers when using different classifiers. As we can see, random forest achieves the accuracy of 98.83% for sitting posture recognition, while the performance of KNN, Bayes, and integration are 91.79% , 84.11%, and 89.4%, respectively. The classifier "D-Tree" can also achieve high accuracy, which is above 97.15% on average. This result indicates that SitR can successfully recognize different sitting postures through careful tag deployment and effective feature extraction. Generally, the recognition accuracy of the classifier will increase by adjusting the parameters. The average accuracy of KNN and integration is more susceptible by adjusting the parameter. However, the parameter of random forest almost does not affect the accuracy when the number of decision trees is larger than 50. Fig. 13 shows the recognition accuracy of the five classifiers for different training samples. The accuracy of the five classifiers increases with the training samples increases. However, the random forest performs better even with less training samples. According to the above comparison, we use the random forest classifier in the following evaluation.

2) Performance With Different Number of Tags: For multiple tags, when two RFID tags are placed close to each other, mutual coupling will affect the received phase sequence. The distance between adjacent tags should be set more than 5 cm for avoiding the coupling interference. For volunteers

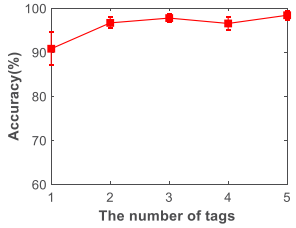

Fig. 14. Accuracy for different number of tags.

of different height, the maximum number of tags that can be pasted is five tags. Therefore, we paste five tags to five different locations of the spine when monitoring the sitting posture. We then arbitrarily select four tags among five tags by using the method of combinations. There are five (C_5^4) combinations, which makes each tag has the opportunity to combine with others. We use the average accuracy of these five combinations to be the result of four tags. Similarly, there are C_5^3 combinations when using three tags, C_5^2 combinations when using two tags, and C_5^1 combinations when using only one tag. The results are also the average accuracy for all the combinations. Fig. 14 shows the average accuracy for different number of tags. The accuracy is high and stable when the number of tags is more than 2. The accuracy is low when using only one tag, which cannot capture enough information for the different sitting postures. The accuracy of using three tags is a little bit higher than the accuracy of using two tags and four tags, except using five tags. Typically, the more tags are used, the higher the recognition accuracy is. However, in order to avoid the mutual coupling interference between tags and provide a comfortable user experience, we aim to minimize the number of tags as much as possible while ensuring high recognition accuracy. Recall that our tag deployment strategy includes

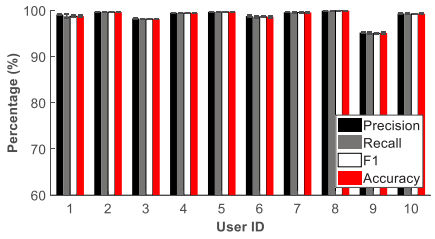

Fig. 15. Recognition accuracy of different users.

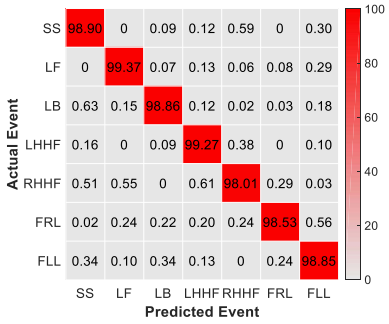

Fig. 16. Confusion matrix of recognition accuracy.

three key regions (i.e., the thoracic, thoracolumbar, and lumbar). Our empirical studies show that pasting one tag within each region is sufficient to capture the effective information for sitting posture recognition and can achieve satisfied accuracy. Besides, the sampling rate of each tag will decrease when the number of tags increases. Based on the above reasons, we choose three tags for sitting posture recognition.

3) Performance Across People: Fig. 15 illustrates the average sitting posture recognition accuracy of ten volunteers, respectively. Among them, there were three volunteers playing computer games during the monitoring period. SitR can achieve high accuracy for each volunteer with an average accuracy of 98.83%. However, the average recognition accuracy of #9 is 95.13%, which is lower than the others. Volunteer #9 kept moving during the monitoring period, and he was the most excited one in volunteers who playing games. To verify if frequent movements reduce the accuracy of sitting posture recognition or not. We added additional sitting posture monitoring for #9 when he used the mobile phone, and the average accuracy increases to 99%. It shows that moving too frequently can affect recognition accuracy. To see the performance of each sitting posture clearly, we further plot the confusion matrix as shown in Fig. 16. Obviously, SitR can recognize SS, LF, LB, LHHF, and FLL very well (the average accuracy of them is 99.05%), while only in some cases, our system cannot distinguish FRL and FLL and confuses RHHF and LHHF.

4) Performance in Different Scenarios: As shown in Table III, we evaluate SitR in two different scenarios with different amounts of multipath effects. The classroom has 12 tables, while the office has 20 tables. One-third of the tables in the classroom lean against the wall, while all tables in the office are placed close to the middle. The sizes of the two rooms are 40 m^2 and 70 m^2, respectively. The classroom has more amounts of multipath effects by comparing it with the

TABLE III
RECOGNITION AVERAGE ACCURACY IN DIFFERENT SCENARIOS

Scenario	Accuracy	Size
Classroom	99.17 %	40 m^2
Office	98.74 %	70 m^2

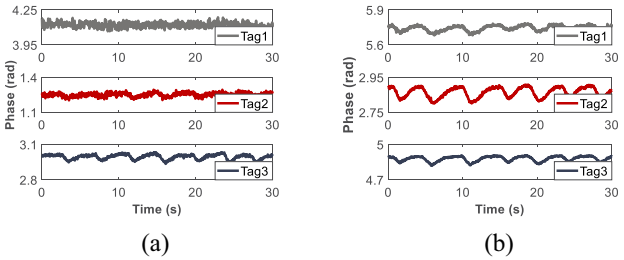

Fig. 17. Phase sequence of different thickness of clothes. (a) Thin clothes. (b) Thick clothes.

office. Obviously, the average accuracy of the two scenarios is around 99%, which indicates that SitR can achieve robust performance in different environments.

5) Performance With Different Thickness of Clothes and the Wrinkle of Clothes: We evaluate the impact of clothing thickness on recognition accuracy. To do so, we use a down coat and T-Shirt to represent thick and thin clothes, respectively. We then ask the same volunteer to wear different thicknesses of clothes for sitting posture monitoring. Fig. 17(a) and (b) shows the measured phase sequence of thin and thick clothes, respectively. We find that the phase change becomes more obvious when wearing the down coat. The primary reason for this interesting phenomenon is that the undulating surface of the thick clothes is larger than that of the thin clothes during human breathing [50]. At the same time, thick clothes usually tend to be closer to the body than thin clothes. So the thick clothes magnify the breathing characteristics by comparing with the thin clothes, which makes the phase change more clearly. Especially, the recognition accuracy is 99.46% for thick clothes and 98.13% for thin clothes. Obviously, thick clothes facilitate the recognition accuracy of the sitting posture.

In order to verify the effect of clothing wrinkles on the phase value and the recognition accuracy, we let three volunteers wear lightweight and wrinkle-prone sun protection clothing. Ten different clothes wrinkles appear when the volunteers put on the sun protection clothes and switches between different sitting postures. The phase offsets caused by these ten different clothes wrinkles range from 0.2 to 1 rad comparing with the case without wrinkle. The wrinkle of clothes cannot affect features related to breath patterns (variance, Pr, range, and DFR) and features in frequency domain (DFR, energy, and entropy). In order to evaluate the effect of clothes wrinkles on the sitting posture recognition, we conduct a 1-h sitting posture monitoring for the three volunteers in the same environment, and the average sitting posture recognition accuracy is about 98.98%. Thus, the wrinkle of clothes has less effect on the recognition accuracy of sitting postures.

6) Performance on Material of Different Chairs and Different Antenna Gains: We choose two kinds of widely used

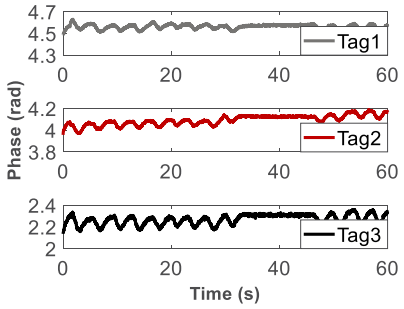

Fig. 18. Abnormal breath detection.

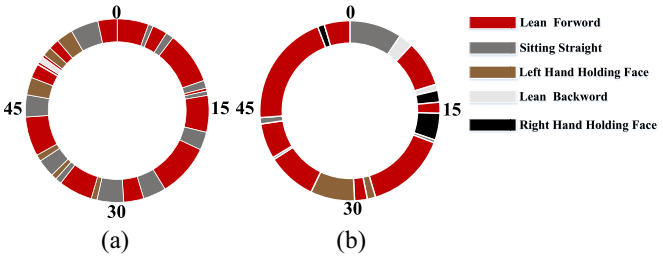

Fig. 19. Sitting postures distribution. (a) #7. (b) #3.

TABLE IV
COMPARISON WITH THE STATE-OF-THE-ART WORK

System	Technique	Method	Posture number	Accuracy
[17]	Video	Faster R-CNN	8	95.6%
[20]	Axis accelerometer	SVM / K-means	5	95.33% / 89.35%
SitR	RFID tags	Random Forest	7	98.83%

chairs with wooden material and plastic material. The back of the wooden chair is straight, while the plastic chair is an ergonomic computer chair with a little arc and conforming to body contours. Both chairs have the same hight and are placed at the same location. The accuracy of the wooden chair and plastic chair is 98.14% and 98.77%, respectively. The result shows that the material of different chairs will not affect the recognition accuracy. Because the two kinds of material will reflect the wireless signal rather than absorb. The reflected signal can be ignored when the tag is close to the antenna.

We evaluate the influence of antenna gains by using two circular polarization directional antennas with 12 and 8 dBi gains. Note that the transmission power and the antenna gain used in this article within the radiation limit value range of the existing router [51]. They achieve the same high accuracy, 99.26% and 98.97%, respectively. The result shows that the antenna gains will not affect the recognize accuracy. Although the antenna gains will not affect the performance, the size of the antenna affects the location where the tag is pasted. The antenna with 8 dBi gains has a smaller size comparing with the antenna with 12 dBi gains. The reader cannot receive the backscattered signal of Tag1 that is pasted higher than the top edge of the antenna, especially for the LB posture. So we need to note the location where is pasted the tag, avoiding the tag is out of the communication range. Antennas with different gains verify the effectiveness of the method in this article. In addition to the sitting posture, the distance between the user's back and the chair's back of other sitting postures are usually 10 cm or more than 10 cm, while the distance of LB is usually very short. It will cause radiation when the back is leaning against the antenna, especially when using a 12-dBi antenna. However, the sitting posture LB is usually maintained for a short time, compared to other sitting postures. Literature [52] shows that the FCC limit is breached between 1 and 10 W radiated power levels at reader antenna to human face distances of 10 cm. The RFID reader used in SitR has 0.25-W radiated power, the SAR versus radiated power at distances of 10 cm will under the FCC limit when we use the RFID antenna with 8 dBi gains. In the future commercialization, we can use 8 dBi gains antennas, or even try smaller gain antennas.

7) Detection of Stand Up and Sit Down Activities: We detect 34 abrupt changes in the phase sequence that caused by standing up and sitting down during the monitoring period. We can successfully identify 33 activities of them by using our activity detection algorithm. Note that we just use the phase sequence of Tag3 to detect the activities. Although the signals from three tags can be received by the reader when the volunteers sit down, Tag1 and Tag2 will lose packets due to exceeding the communication range of the antenna when they stand up.

8) Abnormal Breath Detection: We let one volunteer hold her breath to emulate apnea in the experiment, which approximately lasts 14 s. As shown in Fig. 18, the phase changes of the three tags caused by breathing disappear between 30th and 50th seconds. We can monitor the phase change status of the three tags in real time during the sitting posture monitoring period. It is most likely abnormal breath if the phase changes are tiny or disappeared. Therefore, when apnea occurs, the system can give an alarm immediately.

9) Sitting Posture History for Sedentary People: Fig. 19 shows the sitting postures distribution of sedentary people. We perform sitting posture analysis on volunteers, such as volunteers #3–#7, with 1-h monitoring for random sitting posture. Note that one circle represents 1 h. We obtain the sitting habits of the two volunteers. Volunteer #7 has better sitting habits, with 17.6 min for the SS posture. Conversely, volunteer #3 has a poor sitting habit, with only 6.9 min for the SS posture. Keeping a wrong sitting position for a long time can easily cause health problems, such as musculoskeletal disorders. So users like volunteer #3 need to pay more attention to their sitting posture.

10) Comparison With the State-of-the-Art Work: SitR is the first system that uses wireless signals for sitting posture recognition. The previous works use video-based or wearable sensor-based approaches, whose data type is different with SitR. Therefore, for a fair comparison, we summarize the reported accuracy from each system. Specifically, we compare SitR against system [17] and [20] on the sitting recognition accuracy. System [17] fuses features of the scene and skeletal features extracted from human into semantic features to discriminate eight sitting postures. System [20] uses a single triaxial accelerometer attached on the back of the user's neck to recognize five sitting postures. As shown in Table IV, the accuracy of SitR is 3.23% higher than [17] and 3.5% higher than [20] (comparing with SVM). SitR has a higher

recognition accuracy when recognizes more sitting postures. In addition, SitR is comfortable and does not need any cameras compared to those two works.

VI. Discussion

We discuss some limitations and opportunities for system improvement. For long-term monitoring, the performance of SitR may decrease if we do not update the training set. For example, the accuracy will be decreasing if we use the data collected in the morning as the training set and the data collected in the afternoon as the test set. It is because the same sitting posture becomes more diverse across time. For example, the phase sequence of SS is discrepant at different time periods. However, the phase sequences of seven sitting postures always can be distinguished during the same period of time. In short, long-term monitoring requires updating the data set to ensure a high accuracy. It is still challenging for SitR to recognize the sitting posture across time. We leave this interesting problem as our future work. In future work, we will recognize the sitting posture of multitarget, as well as the fine-grained sitting posture. During the experiment, we attach the antenna to the back of the chair. For commercialization, we can integrate the antenna into the chair in the future, which will be more convenient for people to work or study.

VII. Conclusion

This article introduces SitR, the first sitting posture recognition system using RF signals alone. We demonstrate that with just three tags pasted to the user's back, SitR can successfully recognize seven habitual sitting postures. The experimental results show that SitR can achieve robust and high performance. Our system can further detect the abnormal respiration and provide sitting posture history for sedentary people.

References

[1] F. Lin, L. Ziyi, and L. Chen, "Are you sitting right?-sitting posture recognition using RF signals," in *Proc. IEEE Pac. Rim Conf. Commun. Comput. Signal Process.*, Victoria, BC, Canada, 2019, pp. 1–6.

[2] (2018). *Science Says You've Been Breathing All Wrong. Here's How to Do It Right*. [Online]. Available: https://www.inc.com/wanda-thibodeaux/want-more-energy-focus-try-this-change-to-way-you-brea the.html

[3] (2018). *10 Ways Poor Posture Can Harm Your Health*. [Online]. Available: https://health.usnews.com/wellness/slideshows/10-ways-poor-posture-can-harm-your-health

[4] (2018). *Posture and Breathing: The Physiological Effects of Shallow Breaths*. [Online]. Available: https://www.thebreatheffect.com/posture-breathing-physiological-effects

[5] C. Matthews, K. Chen, and P. Freedson, "Amount of time spent in sedentary behaviors in the united states, 2003–2004," *Amer. J. Epidemiol.*, vol. 167, no. 7, pp. 875–881, 2008.

[6] E. H. Wilhelmina *et al.*, "Flexion and rotation of the trunk and lifting at work are risk factors for low back pain: Results of a prospective cohort study," *Spine*, vol. 25, no. 23, pp. 3087–3092, 2000.

[7] W. Janet, S. Afroditi, D. Mark, C. Jo, L. T. Janice, and R. F. Kenneth, "Objective indicators of physical activity and sedentary time and associations with subjective well-being in adults aged 70 and over," *Int. J. Environ. Res. Public Health*, vol. 11, no. 1, pp. 643–656, 2014.

[8] G. Etienne and H. Wilhelm, "Ergonomics of posture—Review of various problems of standing and sitting posture," *Appl. Ergon.*, vol. 8, no. 3, pp. 135–140, 1977.

[9] C. Swati and W. Wenwu, "Bootstrap averaging for model-based source separation in reverberant conditions," *IEEE Trans. Audio, Speech, Lang. Process.*, vol. 26, no. 4, pp. 806–819, Apr. 2018.

[10] H. Scott and W. Karen, "Impact of seating posture on user comfort and typing performance for people with chronic low back pain," *Int. J. Ind. Ergon.*, vol. 38, no. 1, pp. 35–46, 2008.

[11] O. Kieran, V. Sabine, H. Van Wannes, E. Faik, M. Lien, and D. Wim, "Lumbar repositioning error in sitting: Healthy controls versus people with sitting-related non-specific chronic low back pain (flexion pattern)," *Manual Ther.*, vol. 18, no. 6, pp. 526–532, 2013.

[12] K. Jana, Z. Kristyna, M. Marek, and F. Vera, "Prevalence and risk factors of poor posture in school children in the Czech Republic," *J. School Health*, vol. 77, no. 3, pp. 131–137, 2007.

[13] (2018). *What Are the Main Functions of the Muscular System?* [Online]. Available: https://www.medicalnewstoday.com/articles/321617.php?sr

[14] M. L. Angela, M. B. Katia, K. Hayley, and N. Margareta, "Association between sitting and occupational LBP," *Eur. Spine J.*, vol. 16, no. 2, pp. 283–298, 2007.

[15] S. Edmond, C. Jacky, C. Donald, P. Hubert, C. Yiu-ming, and C. Pong, "Improving posture classification accuracy for depth sensor-based human activity monitoring in smart environments," *Comput. Vis. Image Understand.*, vol. 148, pp. 97–110, Jul. 2016.

[16] Y. Leiyue, M. Weidong, and C. Hao, "A new kinect approach to judge unhealthy sitting posture based on neck angle and torso angle," in *Proc. Int. Conf. Image Graph.*, 2017, pp. 340–350.

[17] M. Weidong, C. Hao, H. Qing, and Z. Fangyuan, "A scene recognition and semantic analysis approach to unhealthy sitting posture detection during screen-reading," *Sensors*, vol. 18, no. 9, p. 3119, 2018.

[18] P. Pujana, N. Chakarida, and M. Pornchai, "Prolonged sitting detection for office workers syndrome prevention using kinect," in *Proc. Int. Conf. Elect. Eng. Electron. Comput. Telecommun. Inf. Technol.*, Nakhon Ratchasima, Thailand, 2014, pp. 1–6.

[19] M. Lan, L. Ke, and W. Chunhong, "A sitting posture surveillance system based on image processing technology," in *Proc. Int. Conf. Comput. Eng. Technol.*, Chengdu, China, 2010, pp. 692–695.

[20] M. Sangyong, C. Woo-Hyeong, Q. Cheng-Hao, and L. Sangmin, "A sitting posture recognition system based on 3 axis accelerometer," in *Proc. IEEE Conf. Comput. Intell. Bioinformat. Comput. Biol. (CIBCB)*, Chiang Mai, Thailand, 2016, pp. 1–3.

[21] E. E. Jheanel and A. V. Larry, "Real-time human sitting posture detection using mobile devices," in *Proc. IEEE Region 10 Symp. (TENSYMP)*, Bali, Indonesia, 2016, pp. 140–144.

[22] M. Corinne, A. Oliver, H. Holger, T. Gerhard, and C. Frank, "Recognizing upper body postures using textile strain sensors," in *Proc. 11th IEEE Int. Symp. Wearable Comput.*, Boston, MA, USA, 2007, pp. 1–8.

[23] H. Yong-Ren and O. Xu-Feng, "Sitting posture detection and recognition using force sensor," in *Proc. 5th Int. Conf. BioMed. Eng. Informat.*, Chongqing, China, 2012, pp. 1117–1121.

[24] M. Congcong, L. Wenfeng, G. Raffaele, and F. Giancarlo, "Posture detection based on smart cushion for wheelchair users," *Sensors*, vol. 17, no. 4, p. 719, 2017.

[25] *Vibocare*. Accessed: Feb. 12, 2019. [Online]. Available: https://www.vibocare.com/

[26] M. Y. Heba Abdelnasser and K. A. Harras, "WiGest: A ubiquitous WiFi-based gesture recognition system," in *Proc. Conf. Comput. Commun. (INFOCOM)*, Kowloon, Hong Kong, 2015, pp. 1472–1480.

[27] A. Q. Mohammed and F. Li, "WiGeR: WiFi-based gesture recognition system," *ISPRS Int. J. Geo Inf.*, vol. 5, no. 6, p. 92, 2016.

[28] J. Shang and J. Wu, "A robust sign language recognition system with multiple Wi-Fi devices," in *Proc. Workshop Mobility Evol. Internet Archit. (MobiArch)*, 2017, pp. 19–24.

[29] A. Virmani and M. Shahzad, "Position and orientation agnostic gesture recognition using WiFi," in *Proc. 15th Annu. Int. Conf. Mobile Syst. Appl. Serv. (MobiSys)*, 2017, pp. 252–264.

[30] K. Ali, A. X. Liu, W. Wang, and M. Shahzad, "Keystroke recognition using WiFi signals," in *Proc. 21st Annu. Int. Conf. Mobile Comput. Netw. (MobiCom)*, 2015, pp. 90–102.

[31] H. Li, W. Yang, J. Wang, Y. Xu, and L. Huang, "WiFinger: Talk to your smart devices with finger-grained gesture," in *Proc. ACM Int. Joint Confe. Pervasive Ubiquitous Comput. (UbiComp)*, 2016, pp. 250–261.

[32] W. Wang, A. X. Liu, M. Shahzad, K. Ling, and S. Lu, "Understanding and modeling of WiFi signal based human activity recognition," in *Proc. 21st Annu. Int. Conf. Mobile Comput. Netw. (MobiCom)*, 2015, pp. 65–76.

[33] Y. Wang, J. Liu, Y. Chen, M. Gruteser, J. Yang, and H. Liu, "E-eyes: Device-free location-oriented activity identification using fine-grained WiFi signatures," in *Proc. 20th Annu. Int. Conf. Mobile Comput. Netw. (MobiCom)*, 2014, pp. 617–628.
[34] W. Teng and Z. Xinyu, "Gyro in the air: Tracking 3D orientation of batteryless Internet-of-Things," in *Proc. 22nd Annu. Int. Conf. Mobile Comput. Netw. (MobiCom)*, 2016, pp. 55–68.
[35] (2019). *Breathing*. [Online]. Available: https://en.wikipedia.org/wiki/Breathing
[36] (2019). *Diaphragmatic Breathing*. [Online]. Available: https://en.wikipedia.org/wiki/Diaphragmatic_breathing
[37] *Posture, Breathing, Body Language and Personal Power*. Accessed: Mar. 6, 2019. [Online]. Available: https://breathing.com/blogs/posture-and-ergonomics/posture-breathing-body-language-and-personal-power
[38] L. Chen, X. Jie, C. Lin, F. Lin, C. Xiaojiang, and F. Dingyi, "Beyond respiration: Contactless sleep sound-activity recognition using RF signals," *Proc. ACM Interact. Mobile Wearable Ubiquitous Technol.*, vol. 3, no. 3, pp. 1–22, 2019.
[39] W. Jue and K. Dina, "Dude, where's my card?: RFID positioning that works with multipath and non-line of sight," *ACM SIGCOMM Comput. Commun. Rev.*, vol. 43, no. 4, pp. 51–62, 2013.
[40] C. Liqiong *et al.*, "RF-copybook: A millimeter level calligraphy copybook based on commodity RFID," *Proc. ACM Interact. Mobile Wearable Ubiquitous Technol.*, vol. 1, p. 128, Jan. 2018.
[41] L. Jinjiang *et al.*, "TagSort: Accurate relative localization exploring RFID phase spectrum matching for Internet of Things," *IEEE Internet Things J.*, vol. 7, no. 1, pp. 389–399, Jan. 2020.
[42] D. Baumgartner *et al.*, "The spinal curvature of three different sitting positions analysed in an open MRI scanner," *Sci. World J.*, vol. 2012, Nov. 2012, Art. no. 184016. [Online]. Available: https://doi.org/10.1100/2012/184016
[43] S. W. Hee, C. O. Jong, and Y. W. Sung, "Effects of asymmetric sitting on spinal balance," *J. Phys. Ther. Sci.*, vol. 28, no. 2, pp. 355–359, 2016.
[44] Z. Jie, T. Zhanyong, L. Meng, F. Dingyi, N. Petteri, and W. Zheng, "CrossSense: Towards cross-site and large-scale WiFi sensing," in *Proc. 24th Annu. Int. Conf. Mobile Comput. Netw. (MobiCom)*, 2018, pp. 305–320.
[45] L. Xuefeng, C. Jiannong, T. Shaojie, W. Jiaqi, and G. Peng, "Contactless respiration monitoring via off-the-shelf WiFi devices," *IEEE Trans. Mobile Comput.*, vol. 15, no. 10, pp. 2466–2479, Oct. 2016.
[46] T. H. Minh, Y. Brosnan, D. Xiaodai, L. Tao, W. Robert, and R. Kishore, "Recurrent neural networks for accurate RSSI indoor localization," *IEEE Internet Things J.*, vol. 6, no. 6, pp. 10639–10651, Dec. 2019.
[47] H. Minh *et al.*, "A soft range limited K-nearest neighbors algorithm for indoor localization enhancement," *IEEE Sensors J.*, vol. 18, no. 24, pp. 10208–10216, Dec. 2018.
[48] L. Chen *et al.*, "RSS distribution-based passive localization and its application in sensor networks," *IEEE Trans. Wireless Commun.*, vol. 15, no. 4, pp. 2883–2895, Apr. 2016.
[49] Z. Jian, B. Hongliang, C. Yanjiao, W. Mingyu, H. Liming, and C. Ligan, "SmartHandwriting: Handwritten Chinese character recognition with smartwatch," *IEEE Internet Things J.*, vol. 7, no. 2, pp. 960–970, Feb. 2020.
[50] C. LiLi *et al.*, "LungTrack: Towards contactless and zero dead-zone respiration monitoring with commodity RFIDs," *Proc. ACM Interact. Mobile Wearable Ubiquitous Technol.*, vol. 3, pp. 1–22, Sep. 2019.
[51] *FCC Rules and Regulations*. Accessed: Jul. 2, 2020. [Online]. Available: https://www.air802.com/fcc-rules-and-regulations.html
[52] D. A. Darmindra and W. E. Daniel, "Impacts of RF radiation on the human body in a passive RFID environment," in *Proc. IEEE Antennas Propag. Soc. Int. Symp.*, San Diego, CA, USA, 2008, pp. 1–4.

Lin Feng received the B.S. degree from Xi'an Shiyou University, Xi'an, China, in 2015, and the M.S. degree from the School of Information Science and Technology, Northwest University, Xi'an, in 2020.

Her past research interests include wireless signal localization, human gesture recognition, and motion tracking.

Ziyi Li received the B.S. degree in software engineering from Northwest University, Xi'an, China, in 2019, where she is currently pursuing the graduation degree with the School of Information Science and Technology.

Her current research interests include wireless signal imaging, human gesture recognition, and wireless sensing.

Chen Liu received the B.S., M.S., and Ph.D. degrees in computer science from Northwest University, Xi'an, China, in 2009, 2012, and 2016, respectively.

She is currently an Engineer with Northwest University and a Postdoctoral Research Fellow with the Department of Electrical and Computer Engineering, University of Victoria, Victoria, BC, Canada. Her research interests include wireless sensing, localization, and wireless networks.

Xiaojiang Chen (Member, IEEE) received the Ph.D. degree in computer software and theory from Northwest University, Xi'an, China, in 2010.

He is currently a Professor with the School of Information Science and Technology, Northwest University. His current research interests include localization and performance issues in wireless ad hoc, mesh, and sensor networks and named data networks.

Xiao Yin is currently pursuing the undergraduation degree with the School of Information Science and Technology, Northwest University, Xi'an, China.

His current research interests include human gesture recognition and wireless sensing.

Dingyi Fang (Member, IEEE) received the Ph.D. degree in technology of computer application from the Northwestern Polytechnic University of China, Xi'an, China, in 2001.

He is currently a Professor with the School of Information Science and Technology, Northwest University, Xi'an. His current research interests include mobile computing, Internet of Things, and information security.